Interactions between deformation, magmatism and hydrothermal activity during active crustal thickening: a field example from Nanga Parbat, Pakistan Himalayas

ROBERT W. H. BUTLER

Department of Earth Sciences, University of Leeds, Leeds, LS2 9JT, UK

NIGEL B. W. HARRIS

AND

ALAN G. WHITTINGTON

Department of Earth Sciences, Open University, Milton Keynes, MK7 6AA, UK

Abstract

The Nanga Parbat massif is a rapidly eroding, thrust-related antiform that is distinct from other regions of the Himalayan orogen in being both intruded by Late Miocene-Pliocene anatectic granites and permeated by a vigorous hydrothermal system. Exhumation is achieved by erosion during thrusting along the Liachar thrust in the apparent absence of extensional tectonics. At depths in excess of 20 km, small batches of leucogranitic melt have been generated by fluid-absent breakdown of muscovite from metapelitic lithologies. These melts ascend several kilometres prior to emplacement, aided by low geothermal gradients at depth and by interaction with meteoric water as they reach shallow levels. At intermediate depths ($\sim$15 km) limited fluid infiltration is restricted to shear zones resulting in localised anatexis. Within the upper 8 km of crust, magmatic and meteoric fluid fluxes are channelised by active structures providing a feedback mechanism for focusing deformation. Leucogranite sheets show a range of pre-full crystallization and high-temperature crystal-plastic textures indicative of strain localisation onto these sheets and away from the country rocks. At subsolidus temperatures meteoric fluids promote strain localisation and may trigger cataclastic deformation. Since near-surface geothermal gradients are unusually steep, the macroscopic transition between distributed shearing and substantial, but localised, cataclastic deformation occurred at amphibolite-facies conditions ($\sim$600°C). Even with the greatest topographic relief in the world, the meteoric system of Nanga Parbat is effectively restricted to the upper 8 km of the crust, strongly controlled by active structures.

KEYWORDS: crustal thickening, deformation, magmatism, hydrothermal activity, Himalayas.

Introduction

DEFORMATION, metamorphism and magmatism resulting from collision tectonics are highly significant processes for reshaping the continental crust. In this contribution we examine the links between deformation and the genesis and emplacement of anatectic granites during active crustal thickening. In particular, we examine the role of active deformation structures in focusing magmatic and hydrothermal fluid systems and we investigate the influence of these fluids on rheological changes in the continental crust.

Young orogenic systems such as the Himalayas offer the best chances of investigating the scale and timing of geological processes. However, one inherent problem in the study of polymetamorphic basement terrains is to identify the fabrics and

Mineralogical Magazine, Vol. 61, February 1997, pp. 37–52

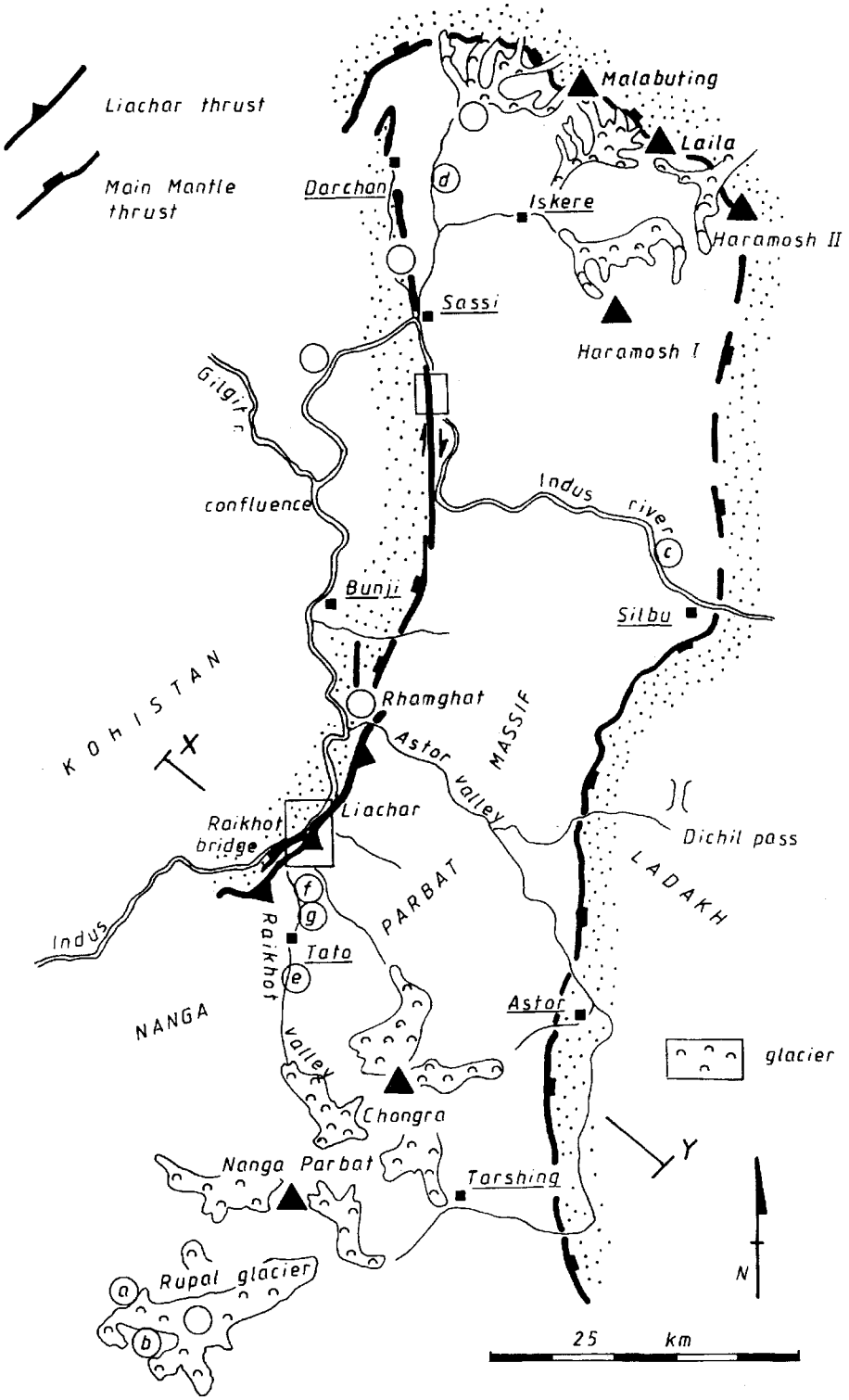
Liachar thrust
Main Mantle thrust
Malabuting
Laila
Darchan
d
Iskere
Haramosh II
Sassi
Haramosh I
Gilgit
confluence
Indus river
c
Bunji
Silbu
KOHISTAN
Rhamghat
Astor valley
MASSIF
Liachar
Raikhot bridge
Dichil pass
LADAKH
f
g
PARBAT
Indus
Raikhot
Tato
e
NANGA
Astor
glacier
valley
Chongra
Y
Nanga Parbat
Tarshing
N
Rupal glacier
a
b
25 km

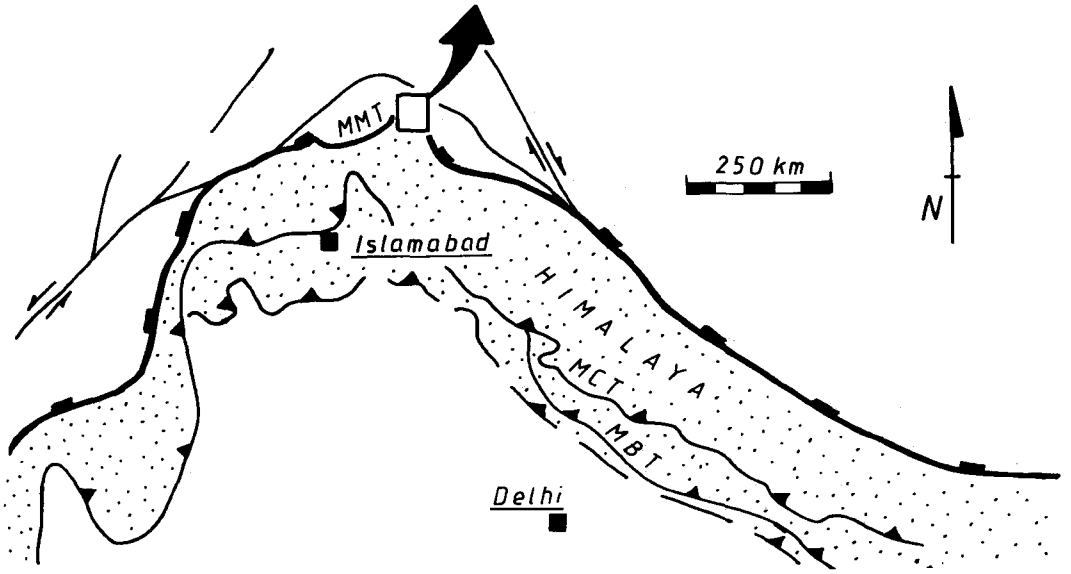

FIG. 1. Location map (left) for the Nanga Parbat massif. X–Y is the section line of Fig. 2. *a-g*, locations of photographs of Fig. 3. Above: NW Himalayas and the site of the Nanga Parbat massif (boxed). The suture zone is marked by the brick-ornament line, Himalayan thrusts with barbs (MMT — Main Mantle thrust, MCT — Main Central thrust, MBT — Main Boundary thrust).

assemblages that are inherited from earlier orogenic episodes. A tacit assumption that underpins many Himalayan studies is that all structures relate to the youngest orogenic episode. For example, much of the work undertaken in the High Himalaya assumes that Miocene leucogranites are derived from nearby migmatites (Deniel *et al.*, 1987). However, there is increasing evidence that migmatisation of the basement occurred during Lower Palaeozoic orogeny, thus greatly pre-dating the Himalayan orogeny (Inger and Harris, 1993; Vance *et al.*, 1996). Clearly any study of polymetamorphic terrains requires that the consequences of earlier orogenic events are distinguished from the most recent metamorphism. Thus our aims in this study of the Nanga Parbat massif are to characterise its basement history, to examine the formation, migration and emplacement of Neogene leucogranites that intrude it, to constrain the timing and scale of meteoric fluid circulation within the massif and to explore links between deformation and the magmatic and meteoric fluid systems.

Geo-tectonic setting

The Nanga Parbat massif is the most northerly outcrop of Indian continental crust within the Himalayan collision zone (Fig. 1). These rocks once formed the footwall to the collision suture, locally named the Main Mantle Thrust (MMT), but have been uplifted through the surrounding overburden (the Kohistan-Ladakh arc) that originally lay in the hanging-wall of the suture. The massif is a high-grade gneiss terrain that contains the youngest granites of the Himalayas. For the past few million years, it has experienced exceptionally rapid cooling (Zeitler, 1985) suggesting that active exhumation rates are very high. Exhumation is achieved by erosion acting upon thrust-related uplift. The youngest structures lie along the western margin of the Nanga Parbat massif. These are exemplified by the Liachar thrust system that carries the massif back across the suture, onto the Kohistan arc and locally over Holocene fluvio-glacial sediments (Butler *et al.*, 1988, 1989). Thus the massif is a large, thrust-related hanging-wall antiform that has been uplifted relative to Kohistan during rejuvenated crustal thickening (Fig. 2). Exhumation occurs by rapid erosion: using the criteria of Wheeler and Butler (1994), there are no major structures recorded that accommodated horizontal extension.

The structurally deepest outcrops in the orogen are exposed in the central and western parts of the massif. Here basement gneisses are intruded by sparse kilometre-sized leucogranite plutons and associated pegmatitic leucogranite sheets. The sheets are syntectonic with respect to the Liachar

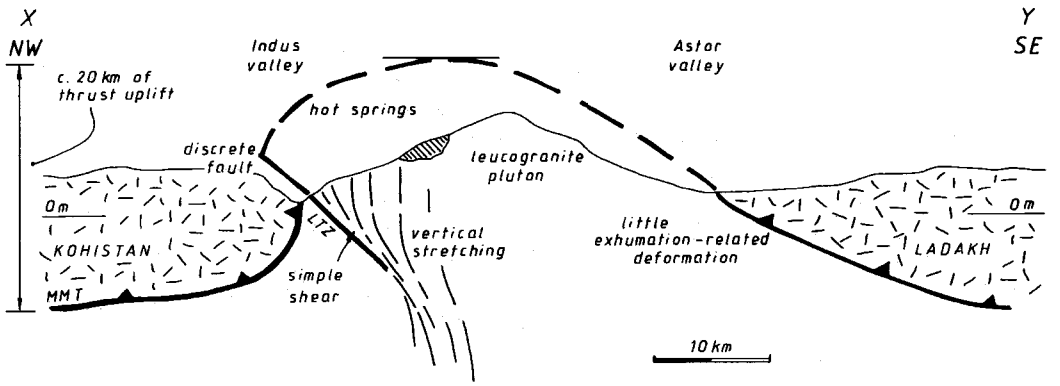

FIG. 2. Schematic cross-section through the Nanga Parbat massif (after Butler *et al.*, 1988), illustrating the style and distribution of exhumation-related structures and their effect on the Main Mantle thrust (MMT), drawn without vertical exaggeration. LTZ - Liachar thrust zone. Section line X-Y from Fig. 1.

thrust. Thus field relations demand that at least some granite genesis occurred in the past few million years, during crustal thickening. This is confirmed by zircon and monazite SHRIMP ages of 7–2 Ma from leucogranite plutons and sheets (Zeitler and Chamberlain, 1991).

The presence of hot springs within the massif, together with skarns and altered fault rocks in the basement, indicate that hydrothermal activity has persisted during the recent history of the massif (Butler *et al.*, 1988, Chamberlain *et al.*, 1995). To examine the interactions between magma genesis, migration and the interaction with hydrothermal systems requires detailed knowledge of field relations and a well-defined basement 'stratigraphy' to underpin geochemical studies.

Basement stratigraphy — the initial state

Basement outcrops from the Nanga Parbat massif are characterized by migmatitic metasediments, granite gneisses and largely undeformed leucogranites. It is tempting to link all these lithologies to a principal episode of high-grade metamorphism of late Cenozoic age (e.g. Chamberlain *et al.*, 1995). We believe that this is unlikely to be the case since field evidence suggests a complex history of deformation, metamorphism and magmatism. Clearly Cenozoic events must be distinguished from their precursors if the later geological history is to be understood. Consequently the basement stratigraphy is briefly outlined below.

The most extensive lithology from the Nanga Parbat massif is a monotonous sequence of orthogneisses, commonly with well-developed feldspar augen. However, in several localities these gneisses contain enclaves of finer-grained material (Fig. 3*a*) and, where the foliations are only weakly developed, the bulk lithology is that of a megacrystic biotite granite. These granites are well-exposed with discordant contacts against metasediments, in the upper Rupal area (Figs 1 and 3*b*). In the upper Raikhot valley (Fig. 1) the granite gneiss is apparently concordant with migmatites, both units sharing the same shape fabrics. In the Upper Raikhot area, at Rupal, the Astor and Indus gorges (Fig. 1), the main location fabric (gneissic banding) is cut by amphibolite sheets (Fig. 3*c*; Butler and Prior, 1988; Butler *et al.*, 1992; Wheeler *et al.* 1995). Since basic magmatism during the Tertiary is unknown throughout the Himalayan orogen, it seems likely that the amphibolites represent a period of pre-Himalayan basaltic magmatism. At Raikhot bridge, in the footwall to the MMT and the Liachar thrust (Fig. 1), the amphibolites intrude and cut the main shape fabric in the augen gneiss. In the Indus gorge the amphibolites cross-cut a high-temperature, migmatitic fabric (Wheeler *et al.*, 1995). Nowhere have they been found to cross deformation fabrics associated with the MMT (Butler and Prior, 1988). Clearly the amphibolites represent a critical stratigraphic marker that appears to separate pre-Himalayan fabrics in the basement from the younger structures that concern us. These units exclusively predate leucogranite sheets and larger intrusions.

The leucogranites of Nanga Parbat are tourmaline-rich and coarse-grained. These form kilometre-sized bodies and a swarm of, apparently coeval, sheets. Regardless of the size of intrusion, they are discordant to fabrics in the surrounding gneisses (Fig. 3*d*) and are clearly intrusive and not formed

from *in situ* melting. Far less abundant are cordierite-rich granitic seams or veins (Fig. 3*e*) which are seen to cross-cut all units within the massif, including the leucogranites. The seams have accumulated within small shears developed in the migmatite basement. The next section discusses the likely sources and conditions of formation of both the leucogranites and the cordierite-bearing seams.

Melt formation and metamorphism

Small plutons, about 1–2 km in diameter, of tourmaline-two mica leucogranite are characteristic of the earlier phase of Himalayan granite formation in the massif. These bodies are similar in major-element geochemistry to High Himalayan peraluminous leucogranites (intruded at ~20 Ma) exposed along the length of the Himalaya (Harris and Massey, 1994) even though much younger ages (2.3–7 Ma) are indicated by ion probe studies of accessory phases from the Nanga Parbat leucogranites (Zeitler and Chamberlain, 1991). However, trace-element abundances differ from those of High Himalayan leucogranites in that Rb/Sr ratios are significantly higher as are concentrations of U and Th. (George *et al.*, 1993). Such variations suggest that these granites are small-volume batch melts derived from a pelitic source of unusually radiogenic character.

The temperature dependence of zircon and monazite solubilities into granitic melts allows the concentrations of trace-elements Zr and *LREE* to be used as a measure of liquidus temperatures (Montel, 1993; Harrison and Watson, 1983). Analyses from the Nanga Parbat leucogranites (Table 1) indicate consistent values from both zircon and monazite thermometry indicative of melt temperatures in the range 700–720°C. Melting under these conditions suggests either melting during fluid infiltration or fluid-absent anatexis by the incongruent melting of muscovite. The intrusive nature of these plutons argues against melting during fluid-saturated conditions since such melts are likely to crystallize *in situ*, forming migmatites, rather than ascend through the crust (Stevens and Clemens, 1993; Brown *et al.*, 1995). The influx of fluid to rocks at temperatures well above the vapour-present solidus relaxes the constraint on melt migration but in this case melting would be strictly limited by available fluid volumes.

Further constraints on the melt-forming reaction can be obtained from the trace-element geochemistry of the leucogranites. The systematic relationship of Rb/Sr ratios increasing with decreasing Ba concentrations seen in trace-element geochemistry of the granites (Fig. 4) is indicative of equilibrium between alkali feldspar and melt. This may be achieved either by early fractional crystallisation of alkali feldspar or by fluid-absent melting of muscovite which leads to the formation of peritectic alkali feldspar (Inger and Harris, 1993). Such trends are inconsistent with fluid-present melting, where increased melt fractions and consumption rather than formation of alkali feldspar results in depletion of Ba in the melt at virtually constant Rb/Sr ratios (Harris *et al.*, 1995), as shown by the vector FP on Fig. 4. Fractional crystallization of alkali feldspar from these melts is unlikely, partly because of the absence of cumulates, and partly because alkali feldspar from the leucogranite plutons generally forms large poikilitic grains enclosing plagioclase and hence is a late phase to crystallize. We therefore conclude that the leucogranites result from fluid-absent breakdown of muscovite from a pelitic protolith. Such anatexis generates melts with elevated Rb/Sr ratios and depleted Ba concentrations relative to their sources (Fig. 4).

Sr-isotope systematics can be used to constrain the precise crustal source of the granites (Table 2; Fig. 5). Data from two leucogranite plutons (Jutial and Tato at localities e and d on Fig. 1 respectively) define a narrow range of $^{87}Sr/^{86}Sr$ ratios between 0.87 and 0.90 whereas basement gneisses from the

TABLE 1. Zr and *LREE* abundances of granitic rocks from Nanga Parbat

Sample	Zr (ppm)	*LREE* (ppm)[1]	T_{Zr} (°C)[2]	T_{Mz} (°C)[3]
Tato granite				
E5a/i	60	0.611	713	725
E5a/ii	62	0.584	712	715
E64	44	0.509	690	711
Z66A	70	0.664	722	726
E70A	74	0.538	723	728
E111	76	0.605	728	718
Z140	81	0.694	731	725
Z141	66	0.614	717	719
Cordierite seams				
Z42/i	7	0.108	575	612
Z42(IV)	8	0.130	585	630
Z45B	29	0.287	664	679
Z46C/i	32	0.198	689	691
Z46C/iv	52	0.247	704	665
Z130a/i	18	0.276	629	667
Z130b/i	26	1.562	654	806
Z130C	14	0.207	615	654
Z130d	18	0.271	625	659

[1] $LREE_t = \Sigma(La + Ce + Pr + Sm + Gd)$ in atomic proportions
[2] Zircon thermometer from Harrison and Watson (1983)
[3] Monazite thermometer from Montel (1993)

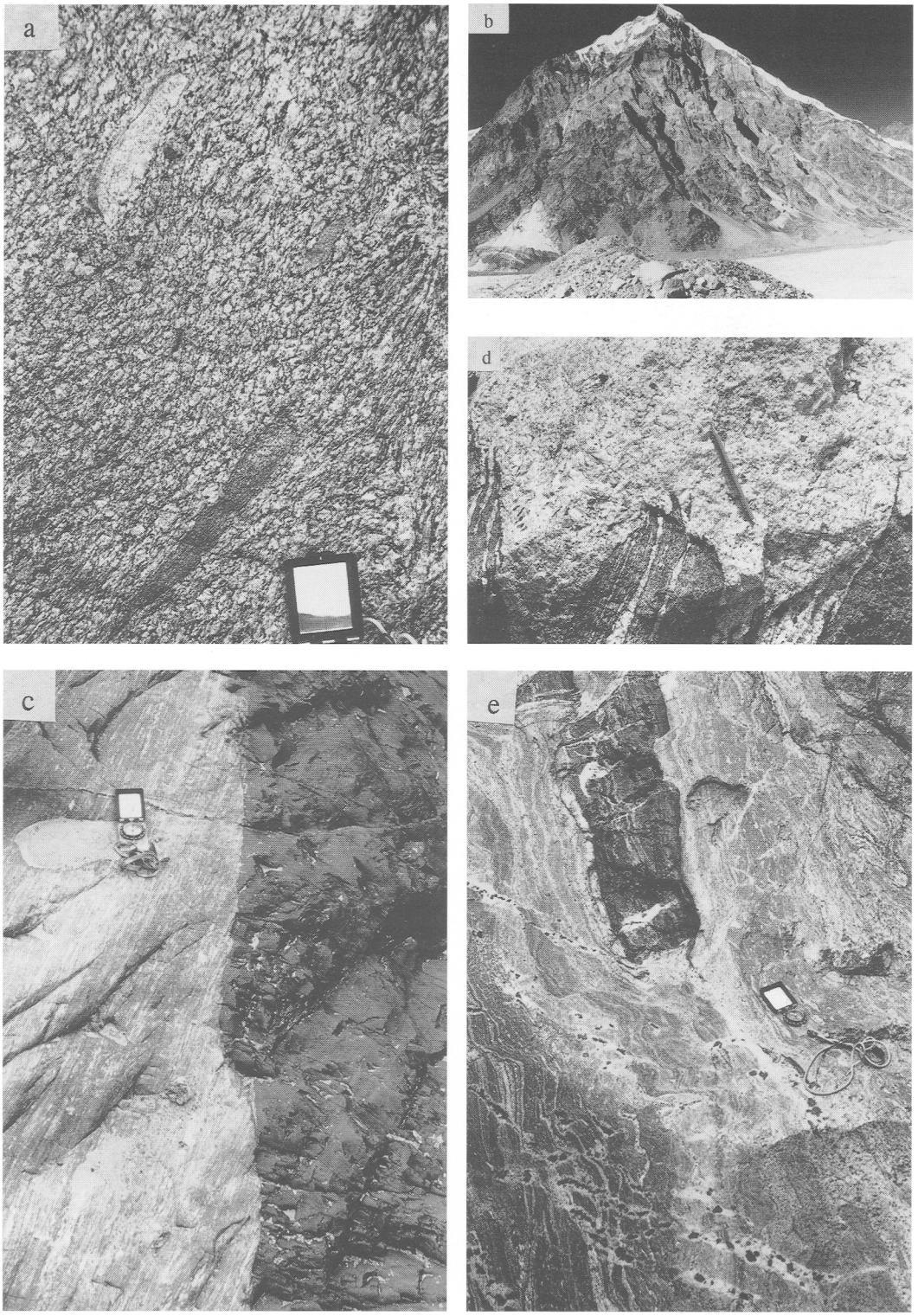
a
b
d
c
e

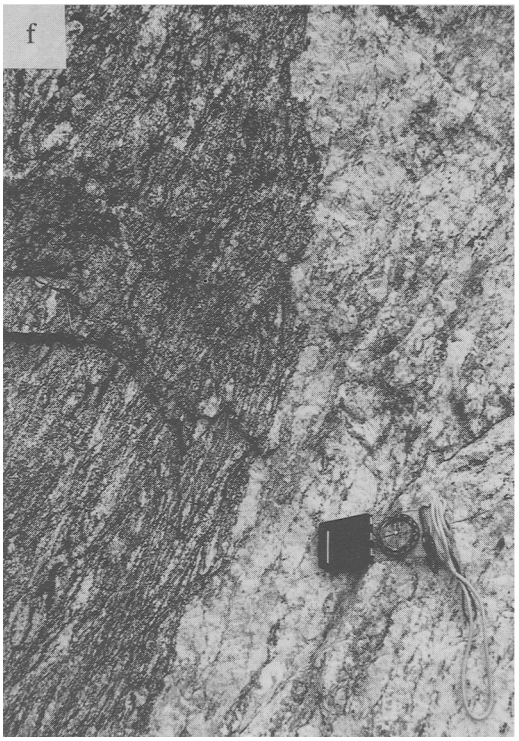

FIG. 3. (*Opposite and above*) Plates of field relationships at Nanga Parbat. Locations given on Fig. 1. (*a*) Biotite, megacrystic feldspar granite with autoliths, the protolith to augen gneiss. Upper Rupal valley. (*b*) View showing pale biotite granites (pre-Himalayan) cross-cutting darker gneisses above the Rupal glacier. The cliffs are about 3000 m high. (*c*) discordant amphibolite sheet cross-cutting gneissic banding, from the Indus gorge. (*d*) Cenozoic leucogranite cross-cutting gneissic banding, Jutial. (*e*) Sub-horizontal cordierite granite seams cross-cutting gneissic banding and vertically stretched amphibolites. Vertical face, viewed to SW, Tato. (*f*) Detail of the margin of Cenozoic leucogranite sheet from the Liachar thrust zone in the Raikhot valley. Note the alignment of fabrics (crystal-plastic deformation) and the localised shear bands that pass from the country rocks (biotite gneisses) into the granite. These shear bands imply top-to-NW shear sense, consistent with other kinematic indicators from the shear zone (Butler and Prior, 1988). Viewed looking SW. (*g*) Macroscopically boudinaged leucogranite sheet from the Liachar shear zone in the Raikhot valley. The granite has an undeformed internal texture indicating deformation occurred pre-complete crystallisation. This feature probably represents a collapsed feeder for tension gashes elsewhere in the shear zone. Viewed to SW.

massif define a broad field from 0.73 to 1.26. These gneisses include orthogneiss, metapsammite and metapelite compositions. The metapelites provide the more fertile mineralogy for melting and generally define a higher $^{87}Sr/^{86}Sr$ ratio (>0.85). Samples of leucogranite sheets cover a range of $^{87}Sr/^{86}Sr$ from 0.87–1.2 and are more variable isotopically than the leucogranite plutons. These results are consistent with formation of the sheets from small-volume bulk melting of a source region with substantial heterogeneity in Sr isotopic composition. The basement gneisses show significant Sr isotopic heterogeneity on the scale of tens of metres down to adjacent hand specimens (George, 1993). Given the preservation of such small-scale isotopic heterogeneities, it is unlikely that pervasive fluid infiltration occurred during melting. While all leucogranites represent low-percentage volume batch melts, the main plutons presumably represent melts formed by somewhat larger melt fractions than the sheets, thus homogenising source heterogeneities and resulting in magmas with a relatively narrow range of isotopic variation. We can conclude that there are sufficiently radiogenic regions of the massif to provide sources for the leucogranites. The likely source is geochemically similar to metapelites within the outcropping

TABLE 2. Rb, Sr, Ba abundances and Rb, Sr isotopic ratios from granites and gneisses from Nanga Parbat

Sample	Rb (ppm)	Sr (ppm)	Ba (ppm)	($^{87}Rb/^{86}Sr$)	($^{87}Sr/^{86}Sr$)	($^{87}Sr/^{86}Sr$) at 5 Ma	error (1 sigma)
Tato pluton							
E5A/i	453	59	164	22.79	0.87732	0.87571	0.00001
E5A/ii	458	60	166	22.46	0.87381	0.87221	0.00001
Z66A	444	58	147	22.69	0.88022	0.87860	0.00001
E70A	395	72	195	16.23	0.88542	0.88427	0.00001
Granite sheet							
Z105	506	22	29	69.16	0.86244	0.85753	0.00001
E81	267	47	79	16.83	0.83808	0.83688	0.00001
E128	545	21	42	78.26	0.88099	0.87544	0.00001
E133	500	33	95	44.65	0.89181	0.88864	0.00001
Cordierite seams							
ZA2/i	341	82	385	12.38	1.00303	1.00215	0.00001
ZA6C/i	185	63	198	8.73	1.03266	1.03204	0.00001
Z130a/i	326	169	884	5.66	0.84665	0.84625	0.00001
Z130b/i	315	177	881	5.22	0.84735	0.84698	0.00001
Z130c	352	172	909	6.06	0.84704	0.84661	0.00001
Z130d	346	187	1020	5.43	0.84644	0.84606	0.00001
Gneiss							
Z130a/ii	258	143	434	5.34	0.84948	0.84910	0.00001
Z130b/ii	273	155	463	5.21	0.85312	0.85275	0.00001

($^{87}Sr/^{86}Sr$) normalised to 0.710230 for NBS-987
($^{87}Sr/^{86}Sr$) for rock standard NBS-607 was measured as 1.200853 ± 0.000016

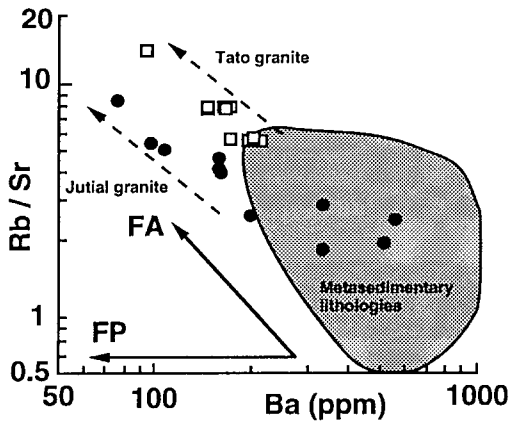

FIG. 4. Rb/Sr versus Ba plot for leucogranite plutons (Jutial=circles; Tato=squares) from Nanga Parbat. Shaded field indicates compositional range of exposed metapelites. Data from George *et al.* (1993) and Table 2. Vectors showing change in trace-element compositions of melt, relative to source, for fluid-absent muscovite melting (FA), assuming 15% muscovite in source, and fluid-present melting of pelites (FP), assuming F = 0.3 (Inger and Harris, 1993).

gneisses but at some greater depth than exposed at present erosional levels. Leucogranite sheets define a wider range of Sr-isotope ratios indicating either a wider range of source compositions, or fluid–melt interactions during the emplacement of the sheets.

Cross-cutting all units within the massif and, consequently, interpreted as being of relatively late development, are rare seams or veins of granitic composition that are rich in cordierite (Fig. 3*e*). These are restricted to the interior of the massif, at least 5 km from unequivocal exhumation structures. When found overprinting gneissic foliation, these seams are developed preferentially along former biotite-rich layers, thus preserving a ghost banding and indicating that biotite is an essential reactant. They are rich in quartz, cordierite and alkali feldspar. The cordierite can occur both as stubby subhedral crystals and as interstitial or xenomorphic grains, both of which are recognised by Harte *et al.* (1991) as textures typical of cordierite formed in small melt pools derived *in situ* from anatectic pelites. The former habit indicates early crystallisation, whilst the latter habit suggests late crystallisation replacing intergranular melt pools. However, major and trace-element analyses of the Nanga Parbat cordierite-bearing seams indicate geochemical variations

inconsistent with a melt origin. Zircon and monazite thermometry yields unrealistic subsolidus temperatures (<650°C; Table 1), and the high proportion of cordierite observed in many seams together with their high silica compositions (SiO_2 >76% in some samples) all suggest that they do not represent pure melt compositions. Rather they are essentially pneumatolytic in origin, probably crystallizing from fluids derived from local anatectic melts. Preliminary Sr-isotope data (Fig. 5) from the seams indicate a wide range of $^{87}Sr/^{86}Sr$ ratios (0.84–1.0) similar to that of the exposed metapelites but quite distinct from the narrow range defined by the main leucogranite bodies. The fluids responsible for their formation are not therefore simply subsolidus fluids derived from leucogranite crystallisation.

Cordierite is not only present in the granite seams but also in many metapelites from the basement gneisses north of Nanga Parbat. Sheaves of sillimanite, ragged biotite and equant spinel all mantled by cordierite are interpreted as anatectic in origin and such textures are well-documented in other anatectic terrains (Srogi *et al.*, 1993). Residual melt pods are observed as granitic leucosomes within the migmatitic gneisses. Such textures reflect dissolution of biotite and sillimanite and nucleation of cordierite with minor spinel. Cordierite and spinel are often closely associated, both representing peritectic phases derived from the melt reaction:

$$\text{Biotite} + \text{Quartz} + \text{Sillimanite} \pm \text{Plagioclase} \pm \text{V} = \text{Melt} + \text{Cordierite/Spinel}$$

Alkali feldspar may be either a reactant or a product of this reaction during fluid-undersaturated melting of pelites depending on the H_2O/K_2O ratio of the melt relative to biotite (Carrington and Watt, 1995). Where present, garnet is seen to be partially replaced by cordierite, indicative of decompression of the pre-anatectic assemblage.

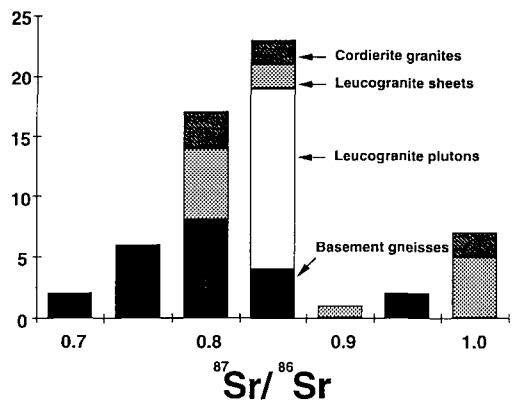

FIG. 5. Histogram of $^{87}Sr/^{86}Sr$ (recalculated at 5 Ma) for basement and intrusive samples from Nanga Parbat. Data from George *et al.* (1993) and Table 2.

Average pressure and temperature estimates derived from a garnet-bearing metapelitic assemblage using THERMOCALC (Holland and Powell, 1990) suggest conditions of 4.4 ± 0.6 kbar, 700 ± 60°C. Garnet is seen to be partially replaced by cordierite in some sections suggesting that estimated pressures may pre-date the time of peak temperature. However, since these metapelites have undergone partial melting, it is likely that *P-T* estimates reflect conditions during, or slightly after, biotite breakdown and melt formation when peak temperatures were experienced and diffusion was enhanced by the presence of an inter-granular melt phase. This inference is confirmed by pressures recorded by the garnet-absent biotite breakdown reaction which, for the observed phase compositions, occurs at 4.6 ± 0.7 kbar at 700 ± 60°C, almost identical to pressures determined from the garnet-present assemblage.

Experimental studies on the anatexis of a natural biotite-sillimanite metapelite at 3–5 kbar (Holtz and Johannes, 1991) determined that melting is initiated between 700 and 800°C depending on the volume of water added to the charge. In these experiments the melt was never saturated with H_2O and so remained fluid-undersaturated even though fluids were needed to trigger melting. Trace-element modelling of the melt reaction in the Nanga Parbat anatectic gneisses suggests a melt fraction of 0.1–0.4 which would require a fluid/rock ratio of 2–7% at 700°C (Holtz and Johannes, 1991). Lower fluid/rock ratios (<1%) result in negligible melt fractions due to the strong partitioning of water into cordierite (Stevens *et al.*, 1995).

Himalayan granite generation in the massif may be summarised as follows. Part of the original protolith of pre-Himalayan metamorphic basement (probably Precambrian migmatites and gneisses) initially underwent partial melting through fluid-absent muscovite breakdown, at temperatures of 700–720°C. The source metapelites, presumably the unmigmatised relics of the inferred pre-Himalayan anatexis in the massif, must have been at pressures of around 7 kbar for melting to occur on the fluid-absent solidus (Fig. 6). Fluid-absent conditions allowed the melt to ascend through the crust before crystallization. Subsequently local fluid infiltration into biotite-rich metapelites, particularly within shear zones, triggered melting at pressures of around 4–5 kbar leading to anatectic textures in the migmatised pelites and formation of pneumatolytic cordierite-rich seams. Preliminary $\delta^{18}O$ data suggest that this fluid had a meteoric component (Chamberlain *et al.*, 1995).

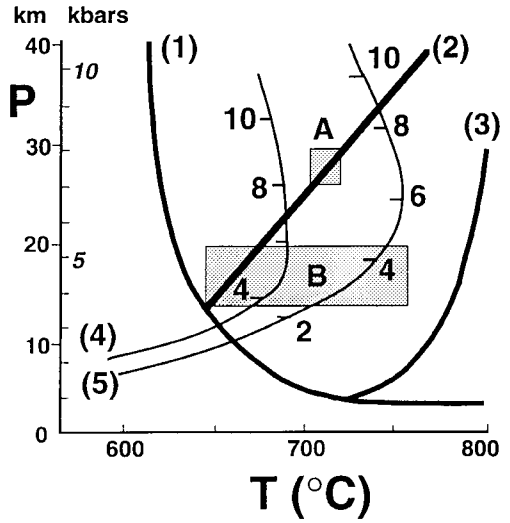

FIG. 6. Pressure-temperature graph of fluid-present solidus for metapelites (1), fluid-absent melting of muscovite (2) and fluid-absent melting of biotite (3). Data from Le Breton and Thompson (1988); Petö (1976). Exhumation paths modelled from Whittington (1996) for lithologies currently exposed (4) and for lithologies currently at depths of 5 km.(5). Numbered ticks indicates time in Ma. Field of leucogranite formation (A) determined from accessory phase thermometry and of basement metamorphism (B) from solid-phase thermobarometry.

Emplacement of leucogranites

The leucogranite plutons at Nanga Parbat migrated to higher structural levels and many leucogranite sheets are emplaced into the active Liachar thrust. Since this magmatic event is synchronous with the Liachar structure, crustal anatexis was probably induced by a combination of high internal heat production (reaching values of 5–7 $\mu W\ m^{-3}$ in the metapelitic lithologies; George *et al.*, 1993) and rapid exhumation by erosion during crustal thickening (Whittington, 1996). In contrast the cordierite granite seams result from fluid infiltration along shear zones. This also triggered anatexis of metapelites. The shears accommodate vertical stretching, in their present orientation, again indicating melting during active crustal thickening. The main leucogranites have migrated from their sources while the small cordierite granite seams have crystallized virtually *in situ*.

Deformation controls not only the chemistry of granitic melts by governing the availability of hydrothermal fluid but also the emplacement and crystallization of leucogranites in the Liachar thrust zone. Within the thrust zone, the leucogranites are emplaced into tension gashes and can be boudinaged. Some leucogranites are penetratively deformed (indicating subsolidus deformation), as indicated by intense fabrics defined by feldspar and quartz (Fig. 3*f*). Others have deformed macroscopic shapes but no internal fabric, indicating that deformation occurred prior to the complete crystallization of the leucogranite (Fig. 3*g*). We interpret these relationships as an indication that deformation continued during the initial stages of crystallisation but terminated prior to complete crystallisation of the melt. In these examples the sheets show marked compositional variation between boudin and necks. These sheets are commonly pegmatitic and have marked trace-element and isotopic heterogeneities. (George *et al.*, 1993). This may suggest that crystallisation was accompanied by the introduction of external hydrothermal fluids which is consistent with their wide ranging Sr-isotope compositions (Fig. 5).

Exhumation and uplift of the massif

It is well established that the exhumation rate of the Nanga Parbat massif is unusually high (Zeitler, 1985), although its precise value remains controversial. Thermal modelling, that takes into account many of the problems involved in modelling rapidly exhumed terrains, such as the telescoping of isograds as they approach the surface, indicates that *P-T* fields determined from thermobarometry can best be reconciled with available isotopic constraints for average exhumation rates of 3.5 km/Ma over the past 10 Ma (Whittington, 1996). Crustal rocks will cross the fluid-absent solidus by near-isothermal decompression. The *P-T* path of outcrops currently exposed from the heart of the massif are shown in Fig. 6 together with the projected path for lithologies at present-day depths of 5 km. It can be seen that whereas melts formed from fluid-absent muscovite melting from protoliths now exposed at present-day crustal levels (curve 4) would cross the solidus at temperatures of ~680°C, rocks now at depths of 5 km cross this curve at temperatures of ~740°C (curve 5), in excess of those recorded by accessory phase thermometry. For solidus temperatures in the range 700–720°C (i.e. to pass through box A) the protolith must currently be at depths of 2–4 km. This value provides an estimate of the vertical extent of leucogranite melt migration. It is reassuring that the model predicts that such melts can form at any time during the period 8 to 2 Ma in still-buried sources, depending on reaction kinetics. This compares well with the radiometric age range (7–2 Ma) for the leucogranites.

Metapelitic assemblages from exposures near Tato equilibrated at 640–760°C and 4–5 kbar. This implies that at the time of migmatite formation (about 4 Ma, according to a monazite age from Smith *et al.*, 1994), thermal gradients in the uppermost crust lay between 130°C/kbar and 190°C/kbar. This is consistent with extremely high present-day near surface geotherms inferred from fluid-inclusion studies (Winslow *et al.*, 1994). However other lines of evidence suggest that such high geothermal gradients could not extend to deeper crustal levels. About 25 km of material has been eroded from above the Tato area in the past 10 Ma. This value is obtained by combining the present-day thickness of Kohistan of about 15 km (Malinconico, 1989) with estimates of about 5 km for regional erosion of Kohistan (Zeitler, 1985) and a value of 5 km for erosion of the Nanga Parbat basement determined by the profile shape of the MMT (Butler *et al.*, 1988). Thus following overthrusting of the Nanga Parbat basement by Kohistan, presently exposed rocks resided at 8 kbar (equivalent to 25 km of overburden). At no time in the past 10 Ma did temperatures within the upper crust exceed 800°C, otherwise widespread anatexis would have resulted from the incongruent melting of biotite in metapelitic assemblages. Hence temperatures could not have risen by more than 100°C (between 700–800°C) across the pressure range of 5 to 8 kbar. This implies a thermal gradient at these depth of about 10°C/km or less. We conclude that although the surface geotherm is very steep under Nanga Parbat, at depths equivalent to temperatures above 700°C, the geotherm is comparatively shallow.

The *P-T* modelling illustrates why leucogranites may have migrated substantial distances as rather small melt volumes within the Nanga Parbat gneisses. They came from levels deeper than, and at a time prior to, *in situ* cordierite-bearing seams and thus at temperatures in excess of ~700°C. Since the thermal gradient is shallow at these temperatures, the migration distance that can be travelled is significant.

Scales of meteoric circulation

Our study of granite genesis and metamorphism within the Nanga Parbat massif suggests that leucogranite genesis occurred by small-volume batch melting of a very heterogeneous source region. This region is presumably still buried. Nevertheless, the Sr isotopic heterogeneities within the source region, inferred from leucogranite compositions, and those measured within the outcropping parts of the massif, strongly suggest that the gneisses have not experienced substantial fluid–rock interactions at depth during their Himalayan history. This is in marked contrast to conditions experienced by the gneisses as they approach the topographic surface. This we can infer not only from the vigorous present-day system of hot springs but also from the observation that rocks within the Liachar shear zone are strongly veined and altered at temperatures below those implied by their peak metamorphic assemblages (Butler *et al.*, 1988). Chamberlain *et al.* (1995) show that the stable-isotope composition of the hot-spring waters are indistinguishable from glacial melt waters sampled from the massif at high elevations. They conclude that the meteoric system has not been diluted by deep-seated metamorphic fluids. However, the evidence for pervasive high-temperature water–rock interaction (500–700°C) is uncertain because it assumes that the mineral textures, and hence phase equilibria, are Himalayan in age. Water–rock interaction certainly occurs at these high temperatures but appears to be channelised on discrete shears resulting in local anatexis of metapelites and the formation of pneumatolytic cordierite-bearing seams. Large-scale pervasive flushing at these depths would have generated large volumes of granite melts, as well as homogenising isotopic compositions in the basement, features for which there is no evidence.

At shallower depths there is evidence of significant fluid infiltration that is focused within the Liachar shear zone. In a study of fluid inclusions from quartz veins within the shear zone, Craw *et al.* (1994) conclude that substantial fluid infiltration occurs at temperatures of about 450°C. They note that the inclusions have high salinities, indicating significant water–rock interaction. This suggests that the fluids were not introduced as short duration pulses, for example during seismogenic pumping (Sibson, 1987). Thus Craw *et al.* conclude that the fluids were entrapped under normal hydrostatic conditions, presumably from a high permeability fracture network. This conclusion accords well with the oxygen isotope data from the spring waters of Chamberlain *et al.* (1995). We concur that meteoric fluid circulation was indeed vigorous at relatively shallow levels; assuming hydrostatic entrapment pressures for the hot fluid inclusions, meteoric waters must penetrate to at least 6 km (Craw *et al.*, 1994).

Interactions between magmatic and meteoric fluid circulation and deformation

But did the meteoric fluid system penetrate deeper? Local percolation into the generation zone for the cordierite 'melts' may be required for their formation. Our pressure estimate of 4.4 ± 0.6 kbar for conditions during anatexis of the exposed metapelites places the depth of fluid penetration during metamorphism between 12 and 15 km. However, this deep system appears to be of minor importance, thus providing a

depth limit to substantial infiltration within the Liachar shear zone. One explanation for this comes from the leucogranite sheets within the shear zone and elsewhere. All the leucogranite sheets, in contrast to the main plutons, are pegmatitic. Chamberlain *et al.* (1995) show that these intrusions have reduced $\delta^{18}O$ values compared with the bulk composition of the gneisses of the massif. We suggest that this anomaly in the oxygen isotopic composition of the granites was caused by interaction between the magma and meteoric water. If true, the rising melts would provide an effective barrier to the lower limits of meteoric water penetration. This barrier could result, not through the ascent of large granite bodies, but through the rising of small volumes within the same narrow, fault-related, pathways used by the meteoric fluids. In contrast, Chamberlain *et al.* suggest that the light $\delta^{18}O$ compositions of the magma were inherited from the melt reaction under the influence of an infiltrated fluid. We note that such fluid-present melting is unable either to result in the observed relationships between Ba and Rb/Sr ratios in the melts (Fig. 4), or to account for the complete segregation between melts and protolith and their ascent to shallower levels.

The dissolution of significant volumes of water into the leucogranite sheets may have been significant for the transport of these magmas. As Brown *et al.* (1995) note, anatexis at the fluid-saturated solidus is likely to promote the retention of a segregated melt due, in part, to the negative gradient of this solidus in *P-T* space (Fig. 6). However, fluid/melt interaction during ascent will enhance migration due to the lowering of melt viscosities. We know that melts have migrated at least 3 km from their source, a minimum estimate of distance constrained by outcrop, and it is likely that the leucogranite melts ascended through a vertical distance of around 2–4 km before final crystallisation as small plutons (Fig. 6). This migration of small melt volumes requires greatly reduced magma viscosities such as would occur by a significant dissolved water component.

Magma ascent in dykes is commonly considered to be fast (Petford *et al.*, 1994). Consequently it could be argued that there is little time for the diffusion of sufficient water through the country rock into the ascending granite liquids to alter their viscosity. Within the Liachar thrust zone there is evidence that, although channelled, the granitic liquids remain molten for significant periods. Many of the syn-tectonic sheets show macroscopically deformed shapes indicating the accumulation of significant tectonic strains. However, these sheets do not contain the strong plastic deformation fabrics that might be expected had the magma crystallised prior to these deformations. Therefore melts must have been present long enough to accumulate significant tectonic strains prior to freezing. During this period water dissolution into the magma would decrease its viscosity, permitting localisation of strain. This may explain the observation that the main leucogranite plutons are sited away from the active uplift structures and, presumably, the main meteoric fluid pathways. Consequently they could retain relatively high viscosities and may not have migrated so far from their source as the magma batches that entered along fractures into the shear zone. These have the potential for much greater migration through intersecting the meteoric fluid circulation system and so were emplaced as sheets at shallower levels now exposed along the western margin of the massif. Future work is planned to study the feedback between magma and fluid migrations with shear zone rheology using these examples.

Apart from the leucogranite plutons, granites within the massif show evidence for tectonic controls on their orientation. Throughout the central massif, the leucogranite sheets lie within fracture geometries that opened subvertically. This suggests that fracture opening occurred when magma pressure exceeded the vertical load — a situation that would have been facilitated by surface erosion. The intrusion of magma into the fracture constitutes a permanent strain by imposing a vertical stretch (Fig. 7). Vertical stretching is also indicated by the conjugate geometries of the shear zones that host the cordierite-bearing seams (Fig. 7). Structural studies suggest that ductile strains which accommodate vertical stretching relate to pure shear shortening (Butler *et al.*, 1989), presumably the principal deformation style at depth since these represent the earliest, hottest deformation structures. Thus both leucogranite sheets and cordierite granite seams have apparently taken advantage of the strain field within the massif.

At shallower crustal levels, the deformation associated with uplift of the massif appears to be focused on the present western margin as a zone of overthrust shear. Leucogranites within the Liachar shear zone occupy tension gashes linking zones of more localised, high shear strain (Butler and Prior, 1988). Although simple shear strains overprint the pure shear, vertical stretching (the converse style) has not been recognised. This supports the overall hypothesis that deeper structural levels deform by pure shear while the shallower levels deform by predominantly simple shear.

Butler and Prior (1988) noted a sharp transition between amphibolite-facies ductile shear fabrics and cataclastic deformation within the Liachar shear zone with little evidence for low-temperature mylonites. This signifies an abrupt change in deformation mode from ductile shearing above $\sim 500°C$ to cataclastic faulting. It is interesting to note that this transition

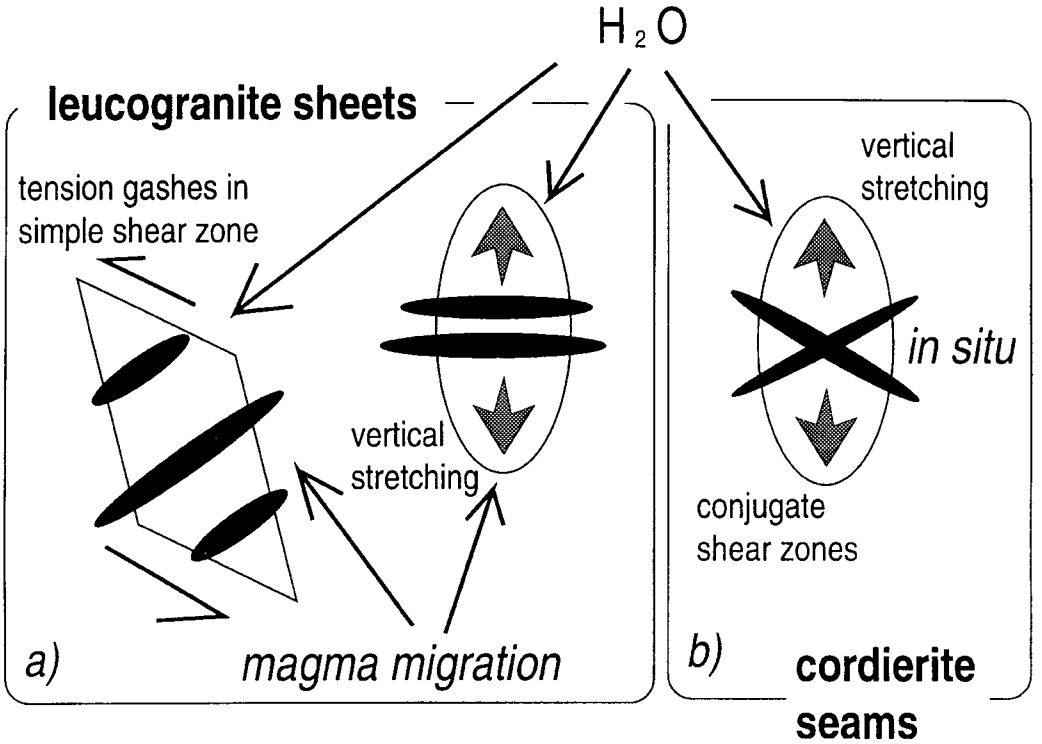

FIG. 7. Tectonic controls on granite emplacement within the massif. (*a*) The leucogranite sheets have migrated into their final sites within tension gashes along the Liachar shear zone or subhorizontal fractures (indicating vertical stretching) towards the centre of the massif. (*b*) The *in situ* melting of metapelites during fluid infiltration and formation of cordierite granite seams occur on sub-horizontal and conjugate arrays indicating vertical stretching.

coincides with the upper range of fluid-inclusion entrapment temperatures for meteoric waters in the shear zone (Craw *et al.*, 1994). We infer that fluid migration to temperatures of 450–500°C enhances the transition between ductile to cataclastic deformation, a transition that will further enhance fluid penetration.

The principal controlling factors for cataclastic deformation are strain rate and confining pressure (Schmid, 1982). Under conventional, far-field deformation rates (convergence of 1–10 cm a^{-1}), confining pressures equivalent to burial depths of less than 8–12 km are needed, most earthquakes on thrusts occurring at about these focal depths. In regions of conventional geothermal gradients, the depth limit for appreciable cataclastic faulting will occur at about 300–350°C. At Nanga Parbat, where the geotherm is greatly enhanced in comparison with other thrust belts, the transitional temperature range is 450–500°C. Consequently, meteoric fluids are able to penetrate into unusually hot rocks (Fig. 8).

Conclusions

The Nanga Parbat massif is a rapidly eroding terrain uplifted by thrusting. The massif is, for the most part, dominated by pre-Himalayan (probably Lower Palaeozoic) fabrics that have been reworked at least locally by Cenozoic deformation. The preservation of early fabrics suggests that the terrain has not experienced pervasive fluid circulation during its recent uplift. Rather, the deep levels of the massif are characterised by anatexis and expulsion of small batches of granitic magma generated by vapour-absent decompression melting. These are represented by the net-vein complex of leucogranite sheets and pegmatites together with rare kilometre-sized plutons. There is evidence for substantial, recharged fluid circulation only within the upper 8 km of the crust, where vigorous hydrothermal circulation is driven by meteoric charge. The evidence for the deepest penetration of possible meteoric waters is recorded by local anatexis of exposed metapelites with associated

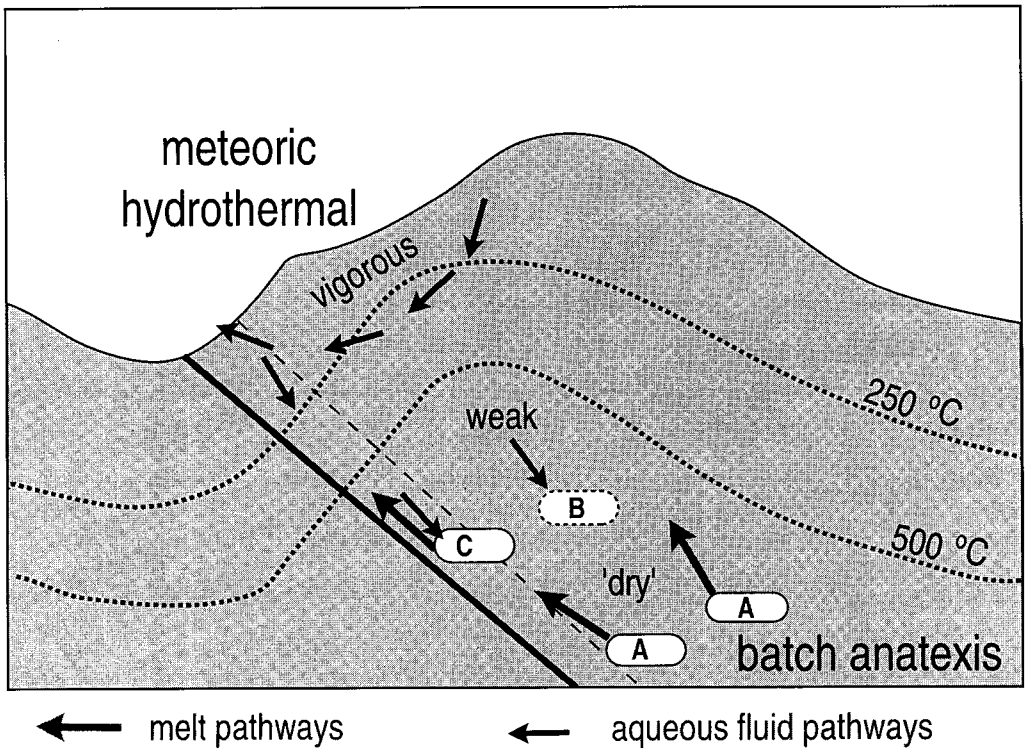

FIG. 8. Cartoon summary of the principal conclusions relating to this study. (*a*) The deep levels of the massif are characterised by low melt-fraction batch melting under fluid-absent conditions to generate leucogranites (sites A). These migrate away from source to be emplaced into tectonically controlled sites (see Fig. 7), in zones of vertical stretching (site B) or simple shear within the Liachar thrust zone (site C). At intermediate depths weak penetration by meteoric fluids allows localised anatexis and formation of cordierite granitic seams within local shears (site B). The meteoric hydrothermal system, although vigorous, does not penetrate deeply and is strongly focussed along active deformation zones where it interacts with rising leucogranite magma (site C).

cordierite-bearing granite seams at depths of 12–15 km. Their formation is distinct from earlier leucogranite formation in that fluid infiltration was required during anatexis. Cordierite-bearing seams are localised, suggesting low fluid/rock ratios, and hence only small volumes of fluids percolating to these depths.

Meteoric fluid circulation and emplacement of melts derived from depth are strongly influenced by coeval deformation structures. Granitic magmas are emplaced into tectonically created fracture networks, locally as tension gashes along syn-uplift thrust zones and pervasively during erosional unloading. These magmas have migrated several kilometres through the crust. Such channelised migration pathways are facilitated by very low geothermal gradients at depth and the incorporation of external fluid during ascent. The lower depth-limit to substantial meteoric charge is probably controlled by the extent of substantial cataclastic faulting on the Liachar thrust zone, estimated at about 8 km depth. The emplacement of leucogranitic melts into the shear zone may also inhibit deep penetration as meteoric fluids are highly soluble in fluid-undersaturated magma. Further work is needed to establish the longevity and timing of fluid migration pathways, particularly within the Liachar thrust system. The present study has shown that even in regions of high topography and resultant strong hydrostatic head, meteorically charged hydrothermal systems are unable to penetrate deeply into the crust and are strongly channelled by active deformation structures.

Acknowledgements

We thank NERC for funding the field research (GR9/1304) and for supporting a Ph.D. studentship (AGW).

We are grateful for thoughtful comments on an earlier draft of the manuscript by John Wheeler and Peter Treloar.

References

Brown, M., Averkin, Y.A., McLennan, E.L. and Sawyer, E.L. (1995) Melt segregation in migmatites. *J. Geophys. Res.*, **100**, 15655–79.

Butler, R.W.H. and Prior, D.J. (1988) Anatomy of a continental subduction zone: the Main Mantle Thrust in northern Pakistan. *Geologische Rundschau*, **77**, 239–55.

Butler, R.W.H., Prior, D.J. and Owen, L.A. (1988) Flashfloods, earthquakes and uplift in the Pakistan Himalayas. *Geology Today*, **4**, 247–50.

Butler, R.W.H., Prior, D.J. and Knipe, R.J. (1989) Neotectonics of the Nanga Parbat syntaxis, Pakistan, and crustal stacking in the northwest Himalayas. *Earth Planet. Sci. Lett.*, **94**, 329–43.

Butler, R.W.H., George, M., Harris, N.B.W., Jones, C., Prior, D.J., Treloar, P.J. and Wheeler, J. (1992) Geology of the northern part of the Nanga Parbat massif, northern Pakistan, and its implications for Himalayan tectonics. *J. Geol. Soc. London*, **149**, 557–67.

Carrington, D.P., and Watt, G.R. (1995) A geochemical and experimental study of the role of K-feldspar during water-undersaturated melting of metapelites. *Chem. Geol.*, **122**, 59–76.

Chamberlain, C.P., Zeitler, P.K., Barnett, D.E., Winslow, D., Poulson, S.R., Leahy, T. and Hammer, J.E. (1995) Active hydrothermal systems during the recent uplift of Nanga Parbat, Pakistan Himalaya. *J. Geophys. Res.*, **100**, 439–53.

Craw, D., Koons, P.O., Winslow, D., Chamberlain, C.P. and Zeitler, P.K. (1994) Boiling fluids in a region of rapid uplift, Nanga Parbat massif, Pakistan. *Earth Planet. Sci. Lett.*, **128**, 169–82.

Deniel, C., Vidal, P., Fernandez, A., Le Fort, P. and Peucat, J.J. (1987) Isotopic study of the Manaslu granite (Nepal Himalaya): Inferences of the age and source of Himalayan leucogranites. *Contrib. Mineral. Petrol.*, **96**, 78–92.

George, M.T. (1993) *The magmatic, thermal and exhumation history of the Nanga Parbat-Haramosh massif, Western Himalaya.* Unpubl. Ph.D. thesis, Open University, Milton Keynes, U.K.

George, M.T., Harris, N.B.W. and Butler, R.W.H. (1993) The tectonic implications of contrasting granite magmatism between the Kohistan island arc and the Nanga Parbat-Haramosh Massif, Pakistan Himalaya. In *Himalayan Tectonics,* (P.J. Treloar and M.P. Searle, eds). *Geol. Soc. Spec. Publ.,* 74, 173–91.

Harris, N. and Massey, J. (1994) Decompression and anatexis of Himalayan metapelites. *Tectonics*, **13**, 1537–46.

Harris, N., Ayres, M. and Massey, J. (1995) The geochemistry of granitic melts produced during the incongruent melting of muscovite: implications for the extraction of Himalayan leucogranite magmas. *J. Geophys. Res.*, **100**, 15,767–77.

Harrison, T.M. and Watson, E.B. 1983) Kinetics of zircon dissolution and zirconium diffusion in granitic melts of variable water content. *Contrib. Mineral. Petrol.*, **84**, 66–72.

Harte, B., Pattison, D.R.M. and Linklater, C.M. (1991) Field relations and petrography of partially melted pelitic and semi-pelitic rocks. In *Equilibrium and Kinetics in Contact Metamorphism*, (G. Voll, J. Topel, D.R.M. Pattison and F. Seifert, eds), 181–473. Springer-Verlag, Berlin, Heidelberg.

Holland, T.J.B. and Powell, R. (1990) An enlarged and updated internally consistent thermodynamic dataset with uncertainties and correlations: the system K_2O-Na_2O-CaO-MgO-MnO-FeO-Fe_2O_3-Al_2O_3-TiO_2-SiO_2-C-H_2-O_2. *J. Metamorphic Geol.*, 8, 89–124.

Holtz, F. and Johannes, W. (1991) Genesis of peraluminous granites 1. Experimental investigation of melt compositions at 3 and 5 kb and various H_2O activities. *J. Petrology*, **32**, 935–58.

Inger, S. and Harris, N. (1993) Geochemical constraints on leucogranite magmatism in the Langtang Valley, Nepal Himalaya. *J. Petrology*, **34**, 345–68.

Le Breton, N. and Thompson, A.B. (1988) Fluid-absent (dehydration) melting of biotite in metapelites in the early stages of crustal anatexis, *Contrib. Mineral. Petrol.*, **99**, 226–37.

Malinconico, L.L. (1989) Crustal thickness estimates for the western Himalayas. In *Tectonics of the Western Himalayas*, (L.L. Malinconico and R.J. Lillie, eds), *Geol. Soc. Amer. Spec. Pap.* **232**, 237–42.

Montel, J.M. (1993) A model for monazite/melt equilibrium and applications to the generation of granitic magmas. *Chem. Geol.*, **110**, 127–46.

Petford, N., Lister, J.R. and Kerr, R.C. (1994) The ascent of felsic magmas in dikes. *Lithos*, **32**, 161–8.

Petö, P. (1976) An experimental investigation of melting relations involving muscovite and paragonite in the silica-saturated portion of the system K_2O-Na_2O-Al_2O_3-SiO_2-H_2O. *Progr. Exper. Petrol.*, **3**, 41–5.

Schmid, S.M. (1982) Microfabric studies as indicators of deformation mechanisms and flow laws operative in mountain building. In: *Mountain Building Processes*, (K.J. Hsu, ed.) 95–110. Academic Press, London.

Sibson, R.H. (1987) Earthquake rupturing as a mineralising agent in hydrothermal systems. *Geology*, **15**, 701–4.

Smith, H.A., Chamberlain, C. P. and Zeitler, P.K. (1994) Timing and denudation of Himalayan metamorphism with the Indian Plate, NW Himalaya, Pakistan. *J. Geol.*, **102**, 493–508.

Srogi, L., Wagner, M.E. and Lutz, T.M. (1993) Dehydration partial melting and disequilibrium in

the granulite-facies Wilmington Complex, Pennsylvania-Delaware Piedmont. *Amer. J. Sci.*, **293**, 405–62.

Stevens, G. and Clemens, J.D. (1993) Fluid-absent melting and the role of fluids in the lithosphere: A slanted summary? *Chem. Geol.*, **108**, 1–17.

Stevens, G., Clemens, J.D. and Droop, G.T.R. (1995) Hydrous cordierite in granulites and crustal magma production. *Geology*, **23**, 925–8.

Vance, D., Oberli, F. and Meier, M. (1996) Pre-Tertiary metamorphic ages from the Zanskar Himalaya. *J. Conf. Abs.*, **1**, 638.

Wheeler, J. and Butler, R.W.H. (1994) Criteria for identifying structures related to true crustal extension in orogens. *J. Struct. Geol.*, **16**, 1023–7.

Wheeler, J., Treloar, P.J. and Potts, G.J. (1995) Structural and metamorphic exolution of the Nanga Parbat syntaxis, Pakistan Himalayas, on the Indus gorge transect: the importance of early events. *Geol. J.*, **30**, 349–71.

Whittington, A.G. (1996) Exhumation overrated at Nanga Parbat, Northern Pakistan. *Tectonophysics*, **260**, 215–26.

Winslow, D.M., Zeitler, P.K. and Chamberlain, C.P. (1994) Direct evidence for a steepened geotherm under conditions of rapid denudation, Pakistan Himalayas. *Geology*, **22**, 1075–8.

Zeitler, P.K. (1985) Cooling history of the NW Himalaya, Pakistan. *Tectonics*, **4**, 127–51.

Zeitler, P.K. and Chamberlain, C.P. (1991) Petrogenetic and tectonic significance of young leucogranites from the northwestern Himalaya, Pakistan. *Tectonics*, **10**, 729–41.

[*Manuscript received 29 November 1995: revised 16 April 1996*]